Materials Research Proceedings 41 (2024) 1099-1105 https://doi.org/10.21741/9781644903131-121

Insights from crystal-plasticity-based predictions on deformation of an Mg-10Gd extrudate

STEGLICH Dirk[1,a *], JEONG Youngung[2,b] and ANDAR Mohammad Omar[3,c]

[1]Institute of Material Systems Modeling, Helmholtz-Centre Hereon, Geesthacht, Germany

[2]School of Materials Science and Engineering, Changwon National University, Changwon, Republic of Korea

[3]GIZ, Dag-Hammarskjöld-Weg 1-5, 65760 Eschborn, Germany

[a]dirk.steglich@hereon.de, [b]yjeong@changwon.ac.kr, [c]andaromar@gmail.com

Keywords: Anisotropy, Plastic Work Contour, Differential Hardening

Abstract. The mechanical behaviour of an extruded magnesium alloy was quantified in tension and compression along the extrusion direction. With the aid of EBSD measurements the material symmetry was examined, and discrete grain orientations were used to predict the multiaxial plastic behaviour along orientations perpendicular to the extrusion direction by means of the ΔEVPSC formalism. It was found that the material is transversely isotropic, shows a small amount of distortional hardening and modest differences in hardening between the extrusion direction and the tangential direction. A phenomenological plasticity law was calibrated based on the predictions, which allowed performing the finite-element analysis of the expansion process of a vascular stent.

Introduction

Mg alloys are promising candidates for biodegradable medical implants. Examples of such devices include cardiovascular or temporary orthopaedic fixtures that are required in the body only for the time of healing [1]. These devices are machined from extruded rods showing anisotropic mechanical properties. Hence, additional to the commonly performed mechanical characterisation along the extrusion direction (ED), other loading directions should be considered. The specific loading scenarios expected from a stent during operation involve compression and extension along the circumferential direction, i.e., crimping and expansion (see Fig. 1) by a catheter. Material characteristics under these loading scenarios are difficult to access experimentally as the diameter of the extruded rod amounts to only a few millimetres. Hence, conventional mechanical testing along a direction other than the ED is not feasible in this case.

Several characteristics of magnesium alloys make constitutive modelling challenging:

1) Their low-symmetric hexagonal close-packed structure deformation requires twinning in addition to slip modes in order to accommodate arbitrary deformation.
2) Wrought magnesium alloys usually exhibit strong initial crystallographic texture, which may drastically evolve due to twin-induced reorientation.

These two above-mentioned characteristics may lead to a strength differential (SD) effect [2] and to plastic anisotropy [3], which may further evolve as the applied deformation increases depending on the loading condition. Hence, as mentioned earlier, mechanical tests data acquired along the ED alone cannot completely characterize the anisotropic behaviour of magnesium alloys.

In this study, to estimate the mechanical behaviour along other directions than the ED and under biaxial stress states, numerical simulations using the incremental elasto-visco-plastic self-consistent (ΔEVPSC) scheme [4] were performed. A mean-field crystal plasticity model with elasto-visco-plastic self-consistent formulation bears the advantage of accounting for the crystallographic texture and its evolution; hence the plastic anisotropy induced by dislocation slip

and twin accompanied by grain reorientation is intrinsically considered. The ΔEVPSC model is relatively efficient and capable of capturing various macro-mechanical features reflecting distinctive micro-mechanical mechanisms of magnesium alloys. The polycrystal aggregate was characterised by the initial texture of the as-received sample of magnesium alloy with 10 wt% gadolinium (Mg-10Gd) after extrusion, and the hardening parameters of the slip and twin mechanisms were calibrated by using the mechanical tests along the ED. The anisotropic and multiaxial behaviours of the as-received extruded rod were analysed in terms of the contours of equal plastic work calculated using the ΔEVPSC model. The polycrystal aggregate was subjected to a multiaxial loading in the principal strain space. Material symmetries were identified by analysing the texture at various positions of a sample. These symmetries were exploited with a phenomenological plasticity model. Its parameters were calibrated based on the ΔEVPSC-predicted mechanical behaviour in the space of tangential and axial stress components.

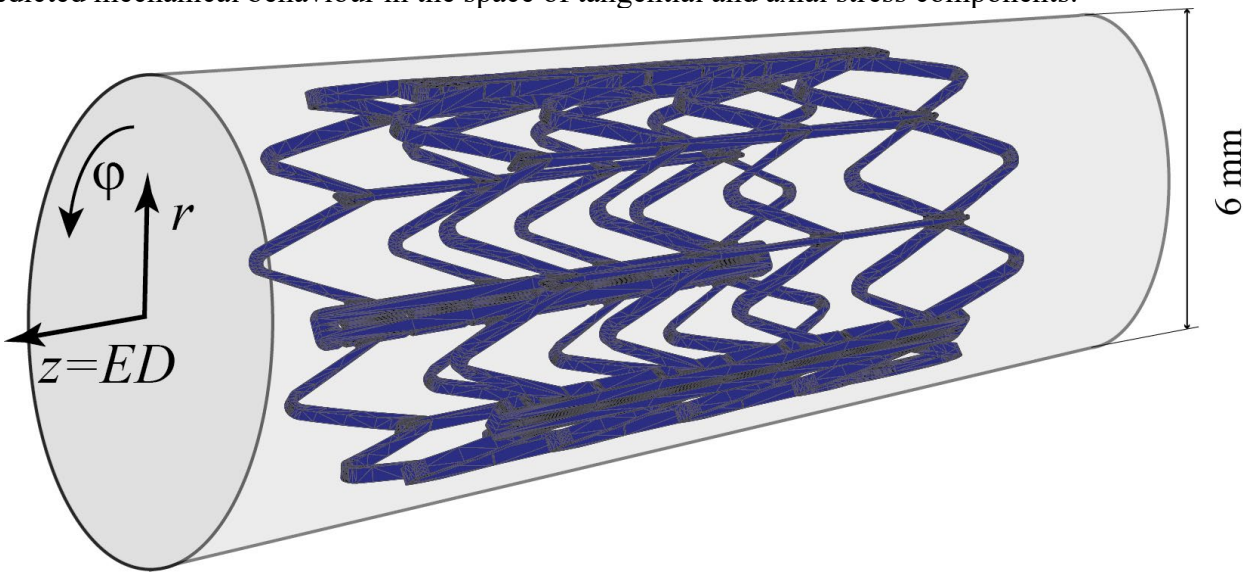

Fig. 1: Vascular stent machined from an extruded rod with its cylindrical coordinates consisting of axes of r, φ, and z.

Material, texture and symmetry

The Mg-10Gd sample was produced by direct chill casting, followed by solid solution heat treatment and in-direct extrusion into a round bar with a 6 mm diameter. Metallographic analyses on its longitudinal section revealed a fully recrystallized grain structure with slightly elongated grains (aspect ratio of 0.57 with the long axis being 12 μm ± 4 μm).

The as-received material appears axisymmetric about the ED. To determine the presence or the absence of such symmetry in terms of the microstructure the crystallographic texture was quantified. To do so, EBSD data obtained at five locations on a circular cross section (plane normal is the ED) were analysed. The chosen five locations include the centre and its neighbouring positions at four φ angles (i.e., φ=0°, 90°, 180°, and 270°). Fig. 2 shows the (0002) pole figures corresponding to the five EBSD scans. The maximum intensity was found at an angle tilted away from the ED towards the radial direction (RD) in all five scans examined. Fig. 2 shows that the texture is heterogeneously developed in the as-received sample. Nevertheless, the overall distribution of crystal c-axis is axisymmetric in the scanned plane. Applying location-specific material behaviour to account for such heterogeneity in texture would make the analysis complicated and is not practical. Therefore, in this study, it was assumed that the overall mechanical behaviour exhibits the transverse isotropy due to the overall axisymmetric texture.

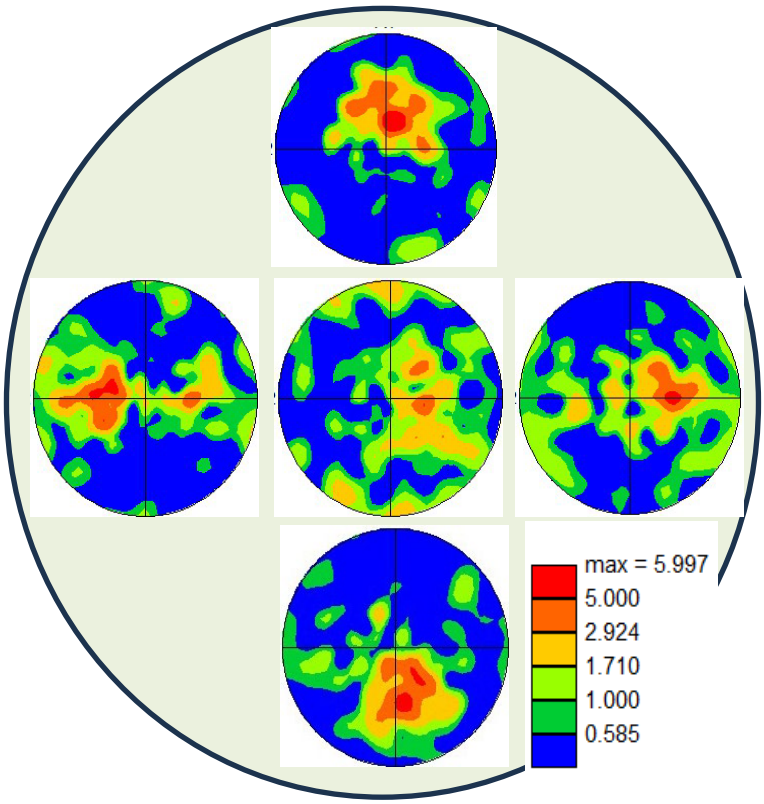

Fig. 2: Basal pole figures obtained at different locations of the extruded rod section.

Prediction of iso-plastic-work contours

The ΔEVPSC framework was used to predict the plastic behaviour in the stress space. For this, the Voce hardening parameters pertaining to basal, prismatic and pyramidal slip modes as well as (extension) twinning mode were calibrated by fitting the uniaxial tensile and the compressive flow responses of the polycrystalline aggregate with the experiments conducted in the ED. The uniaxial tension and compression simulations were performed using a set of 5000 discrete orientations from one of the EBSD scans shown in Fig. 2.

The plastic flow and the hardening behavior obtained from various biaxial loading simulations can be systematically characterized with respect to the specific plastic work W_p. Out of three spatial coordinate axes (r, φ, z), the three different biaxial stress spaces of interest were considered: 1) σ_r vs. σ_φ, 2) σ_z vs σ_r, and 3) σ_φ vs. σ_z. In each 2D biaxial stress space, evolution in the stress components corresponding to a certain plastic work during a proportional strain-ratio-controlled loadings were linearly interpolated. The calculations were repeated under various strain ratios to obtain an iso-work contour as was done in [5]. All the stress coordinates were normalized with respect to its uniaxial tension flow stress, and the results are shown in Fig. 3.

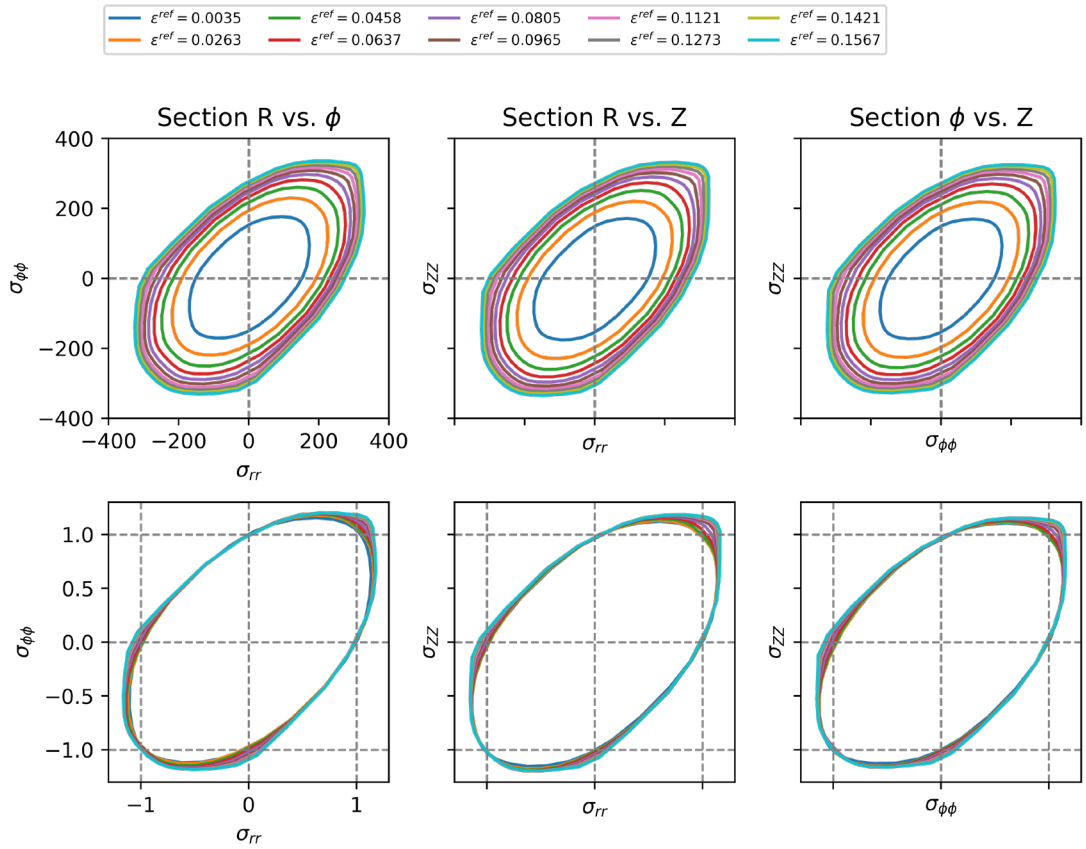

Fig. 3: ΔEVPSC-predicted contours of equal plastic work.

Phenomenological plasticity model

Mean field crystal plasticity models can be used for solving boundary-value problems, from which the plastic work-contours in Fig. 3 were obtained. However, its application to any complex geometry via finite element simulation may not be practical owing to its low computational speed compared to phenomenological plasticity models. In the current investigation, a chosen phenomenological plasticity model was characterized by the results of the ΔEVPSC simulations. Among various phenomenological models, the CPB model developed by Cazacu et al. [6] was selected, which describes the plastic potential as a function of linearly transformed stress tensor via:

$$\bar{B}^a(\boldsymbol{\Sigma}) = (|\Sigma_1| - k\Sigma_1)^a + (|\Sigma_2| - k\Sigma_2)^a + (|\Sigma_3| - k\Sigma_3)^a, \quad (1)$$

where Σ_1, Σ_2, and Σ_3 are the principal values of the transformed stress deviator. The transformed stress deviator $\boldsymbol{\Sigma}$ follows from below linear transformation:

$$\boldsymbol{\Sigma} = \boldsymbol{C}:\boldsymbol{\sigma}. \quad (2)$$

where $\boldsymbol{\sigma}$ and $\boldsymbol{C}$ are the Cauchy stress tensor and the linear transformation matrix. Using the Voigt notation of stress tensor Eq. (2) can be expressed as the following matrix form:

$$\boldsymbol{\Sigma} = \begin{pmatrix} c_{11} & c_{12} & c_{13} & 0 & 0 & 0 \\ c_{12} & c_{11} & c_{13} & 0 & 0 & 0 \\ c_{13} & c_{13} & c_{33} & 0 & 0 & 0 \\ 0 & 0 & 0 & 1/2\,(c_{11}-c_{12}) & 0 & 0 \\ 0 & 0 & 0 & 0 & c_{55} & 0 \\ 0 & 0 & 0 & 0 & 0 & c_{66} \end{pmatrix} \begin{pmatrix} \sigma_r \\ \sigma_\varphi \\ \sigma_z \\ \sigma_{r\varphi} \\ \sigma_{rz} \\ \sigma_{\varphi z} \end{pmatrix}. \quad (3)$$

Due to the global axisymmetry in the texture, a typical loading condition of stents in service would have zero shear components, $\sigma_{rz} = \sigma_{\varphi z} = 0$ in Eq. 3. The latter implies that the parameters c_{55} and c_{66}in Eq. (3) are arbitrary and were set to unity. The remaining four coefficients, c_{11}, c_{12}, c_{13} and c_{33}, were determined by fitting the stress-strain responses obtained from ΔEVPSC simulations for tension and compression along the φ (=r)- and z direction. Isotropic hardening based on two exponential functions was used:

$$\sigma_Y = R_0 + Q_1 \exp(-b_1 p) + Q_2 \exp(-b_2 p), \quad (4)$$

where p is the equivalent plastic strain; and R_0, Q_1, Q_2, b_1 and b_2 are fitting parameters. The results are depicted in the left part of Fig. 4. Right in Fig. 4, the computed initial yield surfaces in the stress space of $(\sigma_\varphi, \sigma_z)$ are shown. The hardening parameters and the transformation matrix $\boldsymbol{C}$ are given in Table 1.

Table 1: Model parameters of the phenomenological plasticity model.

R_0 [MPa]	Q_1 [MPa]	b_1	Q_2 [MPa]	b_2	k	c_{11}	c_{12}	c_{13}	c_{33}
173.9	188.6	14.6	11.2	226.6	0.083	1.42	-0.26	1.34	0.11

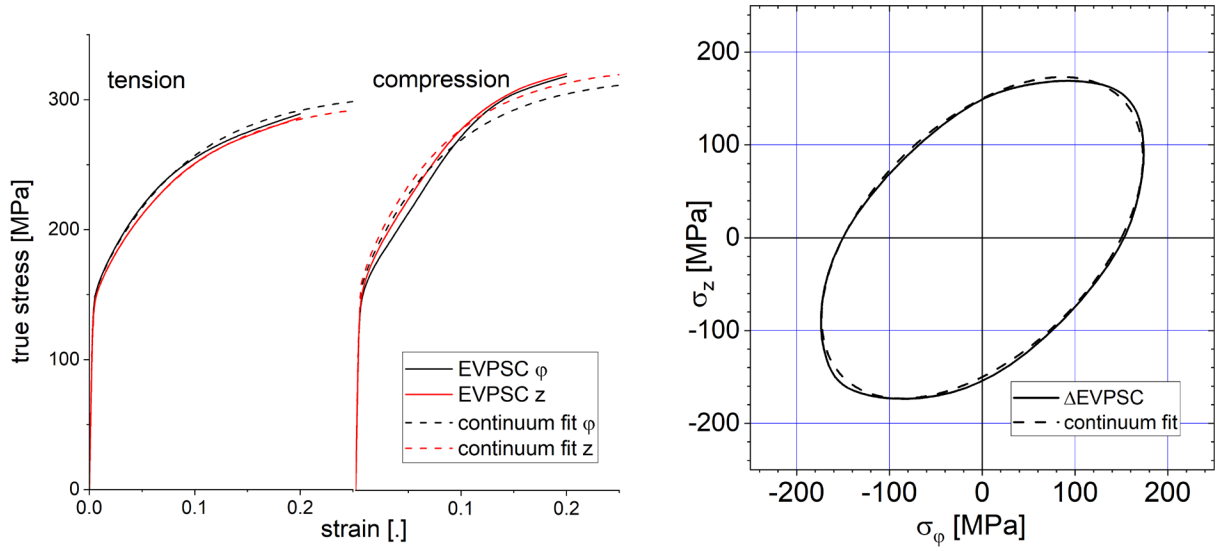

Fig. 4: Flow stress vs. strain curves in tension and compression fitted using the phenomenological plasticity model (left); and the associated initial yield surface (right) in comparison with the ΔEVPSC-predicted initial plastic work-contour.

Results and discussion

The numerical simulations using the ΔEVPSC-model led to the following conclusions:

- The mechanical property of the as-received Mg-10Gd rod exhibits the transverse isotropy on its cross section, which is perpendicular to the ED. The initial iso-work contour in the stress space of (σ_r, σ_φ) is consistent with such symmetry in that the uniaxial tension stresses along r and φ axes are virtually the same.
- The strain hardening behaviour shown in Fig. 4. deviates from the isotropic hardening law:
  i. In the case of tension, while the initial yield stresses along the φ and the z axes are the same, the flow stress σ_φ becomes noticeably higher than σ_z.
  ii. Likewise, compression yield stresses along the φ and the z axes are the same. However, the flow stress σ_z becomes noticeably higher than σ_φ.
  iii. An increased hardening rate is related to a reduction in prismatic slip, which is compensated by a rise of pyramidal slip.
  iv. In equi-biaxial tension, an increased hardening rate is observed, which is related to the decreasing activity of the prismatic slip systems for crystallographic orientations with the c-axis along the ED [7].
- According to the work contour in the (σ_φ, σ_z) plane, the tensile flow stress level in the tangential direction (TD), which aligns with the φ axis, is slightly higher than that in the ED. Under uniaxial compression, the situation is reversed. Consequently, the predicted SD effect, quantified by the ratio of yield stresses in tension and compression (σ_t/σ_c), becomes 1.01 and 0.98 in the TD and the ED, respectively.
- The plasticity law was tailored for this transversely isotropic material while accounting its SD-effect. As a consequence, the yield locus characterized by the phenomenological model in the (σ_r, σ_φ) plane are symmetric about the line $\sigma_r = \sigma_\varphi$, and cannot capture the dissimilarity in the SD effect along the σ_r and σ_φ axes in the stress space calculated by the above-mentioned ΔEVPSC model prediction.
- The respective parameters were determined by fitting the flow curves of the (σ_φ, σ_z) plane in the interval of total strain [0; 0.2]. The anisotropy could be well described. Changes in the mechanisms of deformation due to grain rotation, however, remain a challenge.

The strain hardening features mentioned above in i.-iv. constitute the distortional hardening law. However, the degree of distortion is not pronounced. Therefore, for the application envisaged, distortional hardening was not further accounted for in the phenomenological model considered in this study.

It is frequently reported that adding rare earth elements weakens the texture, which results in reducing anisotropy and tension-compression asymmetry and an increased ductility, e.g. [8]. This could be confirmed for the material under investigation. It remains in the responsibility of the design engineers to decide, when numerically assessing the performance of implants, whether to use a simple isotropic plasticity law or a more complex model that accounts for anisotropy and the SD effect. While the latter might not be essentially required in the present case considering the computational efficiency, other (stronger textured) magnesium alloys might demand for a careful assessment to determine an adequate model to use. In the case of the 3D-simulation of the crimping (reduction of the stent diameter prior to implementation) and expansion (radial extension by an inflating balloon catheter) processes of a typical vascular stent shown in Fig. 5, the computational time increases by a factor of 2.6 if the anisotropic material model is used (ABAQUS software with UMAT interface, 2.2 million degrees of freedom) compared to the case where von Mises plasticity model is considered. The simulation techniques and boundary conditions for the prediction of stents behavior are subject to ongoing research, see e.g. [9].

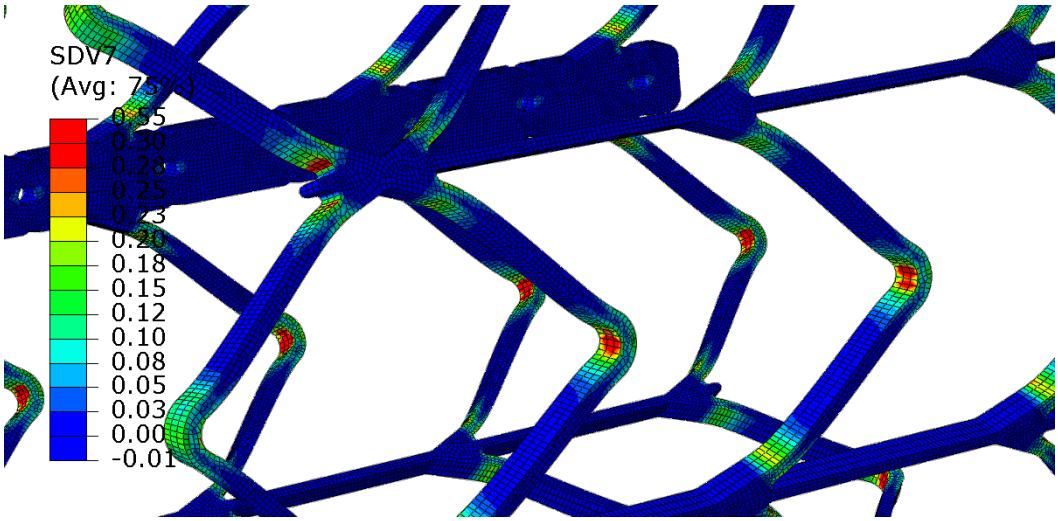

Fig. 5: Equivalent plastic strain in stent segments after crimping and expansion (FE simulation).

Acknowledgements

The authors thank Henry Ovri for conducting the EBSD scans, and Falk Dorn for sample preparation. The fruitful discussion with Holger Aretz regarding symmetry groups is appreciated.

References

[1] Staiger MP, Pietak AM, Huadmai J, Dias G. Magnesium and its alloys as orthopedic biomaterials: A review. Biomaterials. 2006;27(9):1728-34. https://doi.org/10.1016/j.biomaterials.2005.10.003

[2] Hosford WF, Allen TJ. Twinning and directional slip as a cause for a strength differential effect. Metallurgical Transactions. 1973;4(5):1424-5. https://doi.org/10.1007/BF02644545

[3] Kelley EW, Hosford WF. The deformation characteristics of textured magnesium. Trans Metall Soc AIME. 1968;242:654-61.

[4] Jeong Y, Tomé CN. An efficient elasto-visco-plastic self-consistent formulation: Application to steel subjected to loading path changes. International Journal of Plasticity. 2020;135:102812. https://doi.org/10.1016/j.ijplas.2020.102812

[5] Steglich D, Jeong Y, Andar MO, Kuwabara T. Biaxial deformation behaviour of AZ31 magnesium alloy: Crystal-plasticity-based prediction and experimental validation. International Journal of Solids and Structures. 2012;49(25):3551-61. https://doi.org/10.1016/j.ijsolstr.2012.06.017

[6] Cazacu O, Plunkett B, Barlat F. Orthotropic yield criterion for hexagonal closed packed metals. Int J Plast. 2006;22:1171-94. https://doi.org/10.1016/j.ijplas.2005.06.001

[7] Hama T, Takuda H. Crystal plasticity finite-element simulation of work-hardening behavior in a magnesium alloy sheet under biaxial tension. Computational Materials Science. 2012;51(1):156-64. https://doi.org/10.1016/j.commatsci.2011.07.026

[8] Ball EA, Prangnell PB. Tensile-compressive yield asymmetries in high strength wrought magnesium alloys. Scripta Metallurgica et Materiala. 1994;31(2):111-6. https://doi.org/10.1016/0956-716X(94)90159-7

[9] Wiesent L, Schultheiß U, Schmid C, Schratzenstaller T, Nonn A. Experimentally validated simulation of coronary stents considering different dogboning ratios and asymmetric stent positioning. PLOS ONE. 2019;14(10):e0224026. https://doi.org/10.1371/journal.pone.0224026